

Deciphering the Shift from Warm-Dry to Warm-Wet Events in Ice-Covered and Non-Ice-Covered Regions

Xinlu Chen^{1,2}, Lianlian Xu^{1,2}, Ran Yang¹, Ming Cai³, Yi Deng⁴, Deliang Chen⁵, Song Yang^{1,2}, Jiping Liu¹, Qinghua Yang¹, Xiaoming Hu^{*1,2}

1. School of Atmospheric Sciences, Sun Yat-sen University and Southern Marine Science and Engineering Guangdong Laboratory (Zhuhai), Zhuhai, China

2. Guangdong Province Key Laboratory for Climate Change and Natural Disaster Studies, Zhuhai, China

3. Department of Earth, Ocean and Atmospheric Sciences, Florida State University, Tallahassee, FL, USA

4. School of Earth and Atmospheric Sciences, Georgia Institute of Technology, Atlanta, GA, USA

5. Regional Climate Group, Department of Earth Sciences, University of Gothenburg, Gothenburg, Sweden

*** Corresponding authors: Xiaoming Hu**

Email: huxm6@mail.sysu.edu.cn

Submitted to *Geophysical Research Letters*

April 2024

26 Key Points:

- 27 • Warm-dry events prevail in non-ice-covered zones while warm-wet events predominate

28 in ice-covered regions.
- 29 • Duration and frequency of warm-dry and warm-wet events are quantitatively

30 demonstrated for non-ice-covered versus ice-covered regions.
- 31 • Differences in land-atmosphere coupling and the dynamic effect of high-pressure systems

32 cause the paradigm shift.

33

Abstract

Compound warm events exert profound impacts on environment, health, and socioeconomics. A recent study indicated a shift or transition from warm-dry events (WDEs), common in non-ice-covered areas, to warm-wet events (WWEs) in ice-covered zones. Utilizing ERA5 reanalysis data, this study determined the duration and frequency of WDEs and WWEs across ice-covered and non-ice-covered regions. A comprehensive analysis uncovers the physical mechanisms responsible for this shift and attributes it to the weakening of land-atmosphere interaction caused by ice-cover, which inhibits soil moisture feedback and reduces the intensity and duration of warm events in ice-covered areas. Both WDEs and WWEs are associated with high-pressure systems (HPs). WDEs, situated directly beneath HPs, intensify due to adiabatic warming from subsidence motions. Conversely, WWEs, located beneath the poleward fringes of HPs, emerge from advective warming and moistening associated with poleward intrusions of warm-moist air.

Plain Language Summary

Significantly rising temperatures can coincide with extreme weather events such as droughts or rainstorms to form compound warm-dry events (WDEs) or warm-wet events (WWEs), leading to more severe consequences than just hot weather alone. Recent findings indicate that WDEs are more prevalent in non-ice-covered regions where people reside and crops are cultivated, while WWEs are more common in ice-covered areas. This study seeks to comprehend the reasons behind the shift in extreme events by analyzing the conditions during hot summers. Our research has identified two primary causes for the shift. First, in non-ice-covered regions, the ground warms the overlying air, which in turn dries out the soil, leading to even higher temperatures. This explains why more WDEs are observed in these areas. However, in ice-covered regions, this process is inhibited by ice. Secondly, the high-pressure systems accompanying these extreme events behave differently based on the presence or absence of ice. In non-ice-covered regions, these systems are located directly above the regions, exacerbating the hot-dry conditions by pushing air downwards. Conversely, hot-wet conditions occur in ice-covered regions because these areas are situated beneath the poleward fringes of the systems, which transport warm and moist air from the lower latitudes.

1 Introduction

In the recent years, heatwaves have often been observed to coincide with other extremes such as heavy precipitation and droughts, and the compound extremes have received increasing attentions due to their more significant environmental and societal impacts compared to single extremes (Feng et al., 2019; Ridder et al., 2020). The prevalence of warm-dry extremes (including heatwaves and droughts) in populated and cropland areas has been discussed extensively in studies at both regional and global scales (Afroz et al., 2023; Hao et al., 2018; Holmes et al., 2017; Liu & Zhou, 2023a, 2023b; Mueller & Seneviratne, 2012; Xu et al., 2023; Zscheischler & Seneviratne, 2017). Recent extreme warm events, such as the heatwave in central-eastern China (Zhang et al., 2023) and the record-breaking high temperature in Europe (Tripathy & Mishra, 2023), both accompanied by prolonged and severe droughts, caused severe impacts such as energy supply problems, water and electricity shortages, wildfires, and public health risks, thus critically threatening socioeconomic stability (Hao et al., 2022; Salvador et al., 2023). Local land-atmosphere feedback loops (Libonati et al., 2022; Miralles et al., 2019; Zhang et al., 2020) and persistent large-scale atmosphere circulation anomalies (Jiang et al., 2024; Mukherjee et al., 2020) have been considered significant contributing factors to these phenomena.

Heatwaves in extra-polar lands often coincide with dry conditions, whereas those over polar regions tend to synchronize with precipitation. A notable example is the record-breaking high temperatures that occurred over East Antarctica in March 2022, concurrently with heavy precipitation (Clem et al., 2023; Earth, 2022). This warm-wet event was associated with an ‘atmospheric river’, a long and filament-shaped atmospheric structure that transports abundant heat and moisture from the Southern Ocean (Pohl et al., 2021). Similarly nuanced warm-wet events were also observed in West Antarctica (Djoumna & Holland, 2021; Nicolas & Bromwich, 2011), Antarctic Peninsula (Gorodetskaya et al., 2023), and Greenland (Mattingly et al., 2020; Xu et al., 2022), all resulting from the intrusion of heat and moisture. In contrast to the direct effect induced by warm-dry spells on extra-polar lands, the occurrence of warm-wet events may lead to more complex and farer-reaching climate impacts. These events may amplify the vulnerability of ice sheets through extra melting and destabilization of coastal ice, leading to significant ice mass loss and freshwater inflow into the oceans (Hu et al., 2019; Li et al., 2023). Ultimately, these processes contribute to accelerated sea level rise (DeConto & Pollard, 2016; Rignot et al., 2011).

and weakened Atlantic Meridional Overturning Circulation (Bakker et al., 2016; Gao et al., 2024; Zhu et al., 2014). Given the significant impact of warm-wet events on ice-covered regions, Yang et al. (2024) have emphasized that these areas exhibit a much higher synchrony of extreme warm and precipitation events compared to the extra-polar lands, and marked a paradigm shift in our understanding of compound extreme warm events over ice sheets. The study has also indicated that a synchrony may arise from warm-moist air intrusions, as suggested by previous case studies (Gorodetskaya et al., 2023; Shields et al., 2022; Wang et al., 2023; Wille et al., 2024; Xu et al., 2022; Zou et al., 2021).

Systematical studies of the new characteristics and physical mechanisms for compound warm-wet extreme events over ice sheets are also crucial under global warming. On the one hand, the frequency, duration, and intensity of warm events have been increasing (Barriopedro et al., 2023; Feron et al., 2021; González-Herrero et al., 2022); and on the other hand, precipitation process tends to shift from a solid state to a liquid state (Schot et al., 2023; Vignon et al., 2021). The combined effect of these two factors could result in a nonlinearly damaging impact on ice caps (Bintanja, 2018; McNeall et al., 2011). While the individual mechanisms associated with compound warm-dry events have been widely explored, spanning from local processes (Miralles et al., 2019) to large-scale modes of climate variability (Mukherjee et al., 2020; Yang et al., 2024a, 2024b), there is still a lack of systematic analysis of the compound warm-wet events. Moreover, an enhanced understanding of the warm-wet extreme events over polar ice sheets contributes to better identifying the model biases in numerical simulations and improving model simulations and thus forecasting accuracy (Cai et al., 2024; Ridder et al., 2021), especially in the cryosphere due to scarce observations and complex dynamics (Deb et al., 2016; Leeson et al., 2018).

This study, building upon the perspectives proposed by Yang et al. (2024), is aimed to provide robust evidence and physical interpretations for the paradigm shift in compound extreme hot events. First, we examine the proportion and duration of warm-wet events and warm-dry events during summers from 1979 to 2022 in five representative regions: Greenland, West Antarctica, Europe, South China, and the US Great Plains. These regions are identified as the hotspots of research on heatwaves with regard to ice melt, human health risk, and yield loss (Han et al., 2022; He et al., 2022). Secondly, we investigate the relative atmospheric processes and surface energy budget through a composite analysis. More importantly, we quantify and compare the associated

land-air interaction using the coupling metric (Miralles et al., 2012; Seo & Ha, 2022) to provide an improved understanding of the crucial role in triggering the different compound warm events.

2 Data and Methods

2.1 Data

The daily ERA5 reanalysis fields for the summers of 1979-2022 (i.e., June, July, and August for the Northern Hemisphere, and December, January, and February for the Southern Hemisphere) with a horizontal resolution of $1^\circ \times 1^\circ$ are used in this study. These fields are provided by the European Centre for Medium-range Weather Forecasts (Hersbach et al., 2020). The surface variables include 2-m temperature (T), precipitation (P), surface pressure, actual and potential evaporation, soil water, sensible and latent heat fluxes, as well as net and downward fluxes of short-wave radiation (SWR) and long-wave radiation (LWR). Cloud cover and geopotential height, with a vertical resolution of 19 pressure levels extending from 1000 hPa to 1 hPa, are also analyzed.

2.2 Definitions of compound extreme events

The 75th and 25th percentiles of summer daily T and P from 1981 to 2010 are chosen as the thresholds for extremes, denoted as T_{75} , P_{75} , and P_{25} , respectively. These percentiles allow a larger number of events to be selected for analysis (Beniston, 2009). The co-occurrence of heatwaves ($T > T_{75}$) and extreme precipitation ($P > P_{75}$) is defined as warm-wet events (WWEs) at each grid, while the co-occurrence of heatwaves and extreme droughts ($P < P_{25}$) is defined as warm-dry events (WDEs). To identify WWEs or WDEs within an area, we first assign 1 to the grids where events occur and 0 to those where non-events occur on a given day, and then calculate the regional means. The days when the spatial extent exceeds 1 standard deviation are defined as extreme cases. To further explore the mechanisms driving WWEs and WDEs, a composite analysis is applied to the extreme cases. The significance levels for the composite values are determined by the Student's *t*-test.

2.3 Coupling metric

To quantify the strength of land-atmosphere interaction at a given location, a coupling metric (π), related to surface energy flux anomalies and their skill in explaining the variation of temperature (T), was proposed by Miralles et al. (2012) as:

$$\pi = [(R_n - \lambda E)' - (R_n - \lambda E_p)'] \times T'$$

where R_n refers to the surface net radiation, λ is the latent heat of vaporization, and E and E_p denote the actual and potential evaporation, respectively. The primes denote the standardized anomalies deviated from the 1979-2022 climatology. Positive values of π are obtained from the regions where the land-atmosphere interaction is intense. The larger the value of π , the more intense is the land-air interaction.

3 Results

Figure 1 presents the global pattern of the percentage of WWEs days to the total number of WWEs and WDEs days, illustrating the prevalence of compound warm events in summer. The proportion of WWEs exceeds 80% over the polar ice sheets but falls below 20% over most extra-polar lands. This result indicates that the paradigm of compound extremes shifts from WDEs over non-ice-covered zones to WWEs over ice-covered regions. We explore and compare the mechanisms for WWEs and WDEs, focusing on two regions where WWEs prevail, including Greenland (GL) and West Antarctica (WA), as well as three zones dominated by typical WDEs, including Europe (EU), South China (SC) and the US Great Plains (USGP).

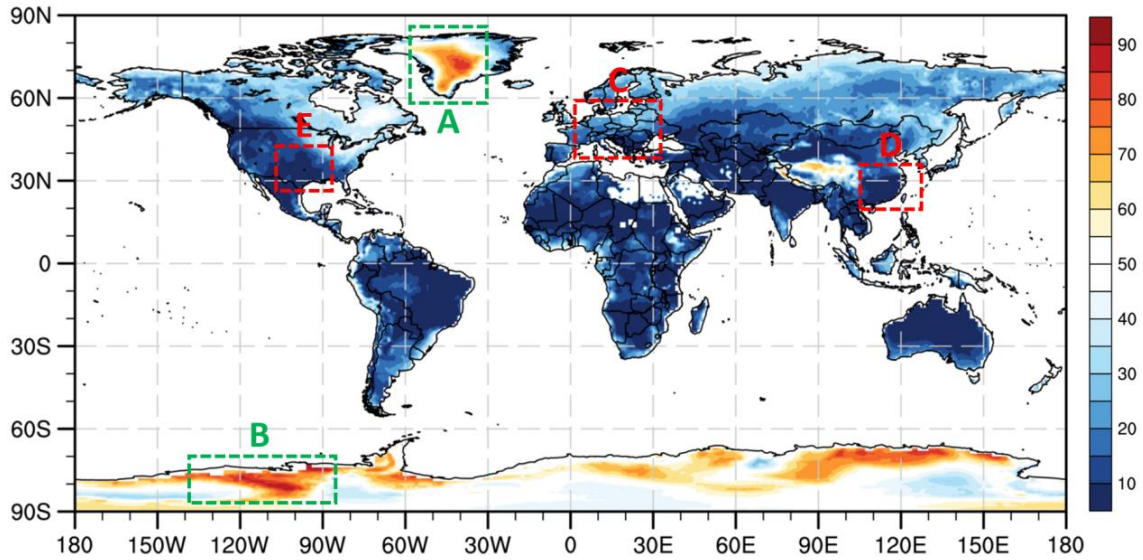


Figure 1. Percentage (units: %) of warm-wet event (WWE) days to the total number of WWE and warm-dry event (WDE) days during summer. The regions labeled A, B, C, D, and E represent Greenland (GL), West Antarctica (WA), Europe (EU), South China (SC), and the US Great Plains

(USGP), respectively. The proportion is calculated as the number of WWE days divided by the total number of WWE and WDE days.

Figure 2 shows the duration of WWEs and WDEs in the above five regions. Short-duration events lasting up to five days account for more than 75% of both WWEs and WDEs, meaning that these two types of events are predominantly short-duration events. There are a few cases that WDEs can last more than 10 days, particularly over EU. However, it is rare for a WWE to last more than 10 days. Overall, WDEs last longer than WWEs.

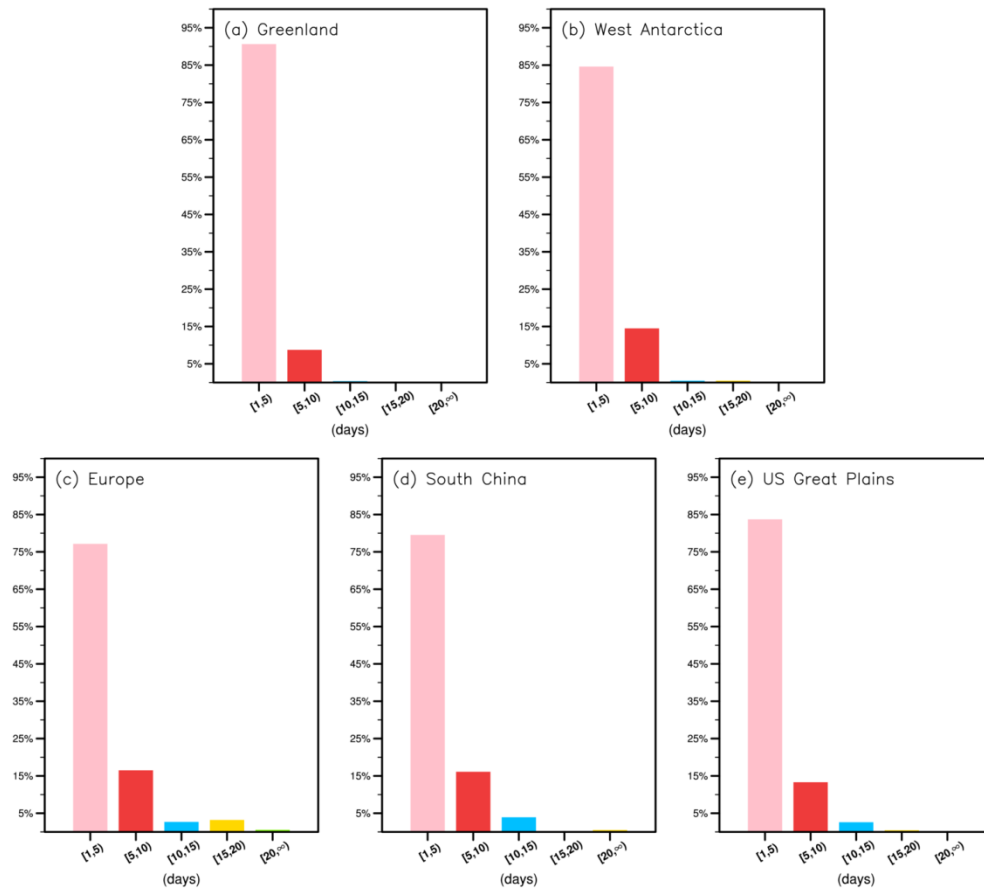


Figure 2. Proportions of (a) WWEs in GL, (b) WWEs in WA, (c) WDEs in EU, (d) WDEs in SC, and (e) WDEs in USGP for different durations.

By definition, the near-surface warming during WWEs in GL and WA occurs in synchrony with increased precipitation, while this does not occur during WDEs in EU, SC and USGP (Fig. 3). During WWEs, robust high-pressure systems (HPs) with a quasi-barotropic vertical structure

185 occur over both GL and WA (Figs. 3u-3v), and the locations of WWEs, indicated by green lines,
186 are at the poleward fringes of HPs. Guided by the poleward circulation associated with
187 anticyclones, large amounts of heat and moisture from the lower latitudes are transported towards
188 the ice sheets. This results in inland warming and, coupled with local elevated elevation, leads to
189 cloud formation (Figs. 3k-3l) and precipitation (Figs. 3f-3g). In the areas where cloud cover
190 increases, the downward SWR supply of energy to the surface decreases (Figs. 4XI-4XII).
191 However, the downward LWR is greatly enhanced, amplifying surface warming over the
192 ice-covered surface (Figs. 4XXI-4XXII).

193 During the WDEs in EU, SC, and USGP, HPs also prevail (Fig. 3). However, in contrast to
194 WWEs, WDEs are located beneath HPs. Convection is suppressed by downdrafts at the center of
195 HPs, precipitation is reduced (Figs. 3h-3j), and clouds are dissipated (Figs. 3m-3o). The former
196 process leads to associated droughts, and the latter creates clear-sky conditions that enhance SWR
197 supply at the surface (Fig. 4). Abnormal SWR is absorbed and heats the ground. Then, more
198 energy is lost via long-wave radiation from the surface to the air and even to the outer space (Figs.
199 4XXVIII-4XXX), as well as via surface latent (Figs. 4III-4V) and sensible heat fluxes (Figs.
200 4VIII-4X). The differences in surface energy budget during WWEs and WDEs indicate that in the
201 polar region, WWEs are driven by anomalous horizontal warm and moist air transport, but in the
202 extra-polar region, the WDEs are driven by anomalous vertical descending motions.

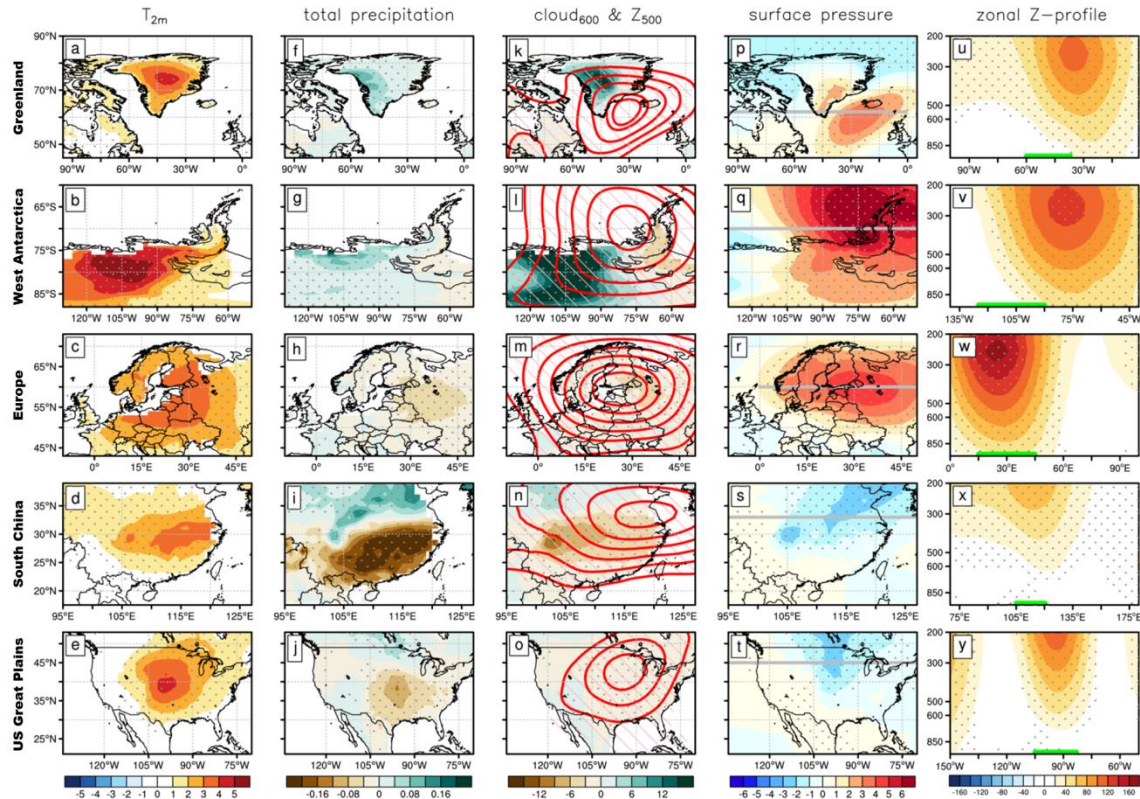


Figure 3. Atmospheric processes associated with the WWEs in GL and WA, and the WDEs in EU, SC and USGP. Shadings represent the daily composite anomaly values of (a-e) 2-m temperature (units: K), (f-j) total precipitation (units: mm), (k-o) 600-hPa cloud cover (shading; units: %), (p-t) surface pressure (units: hPa), and (u-y) height-longitude profile of geopotential height (units: gpm) at the latitudes marked by gray lines in (p-t). Red contours in (k-o) denote positive 500-hPa geopotential height anomalies (units: gpm), with an interval of 15 gpm in (k, l, m, o) and 5 gpm in (n). Gray dots, as well as the pink lines in (k-o), indicate the areas where the anomalies are statistically significant at the 95% confidence level. The green lines in (p-t) denote the main regions of compound extreme events.

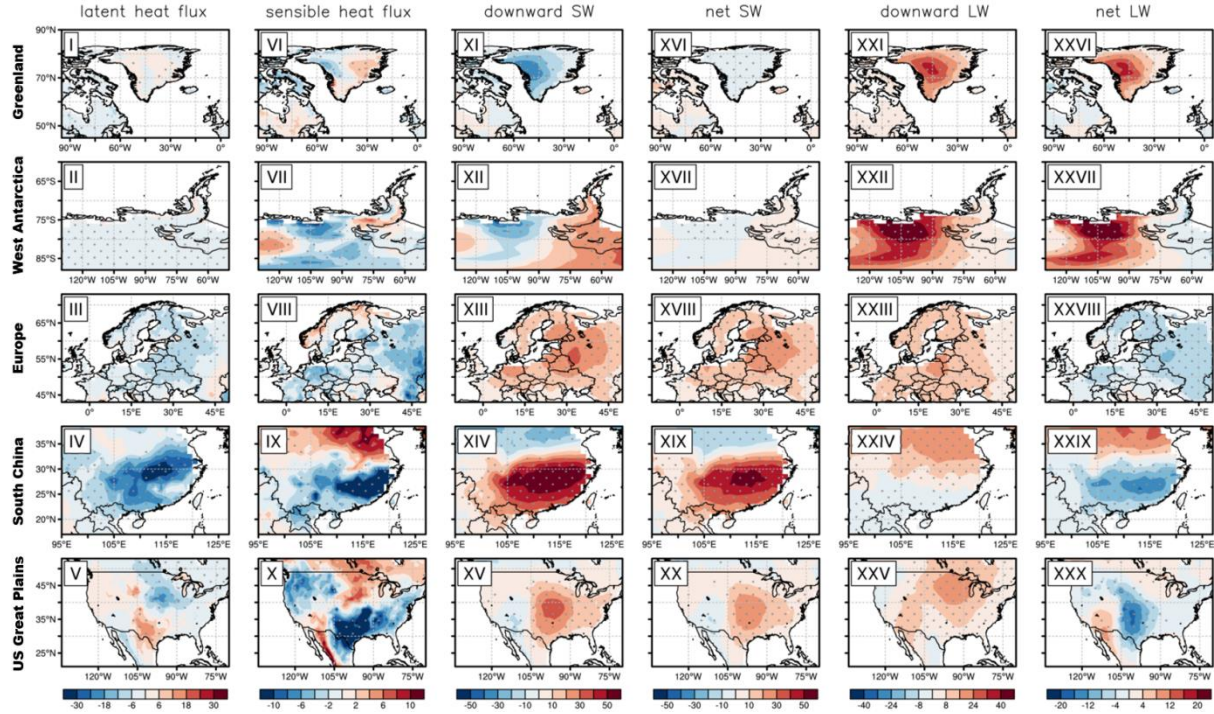


Figure 4. Surface energy budget associated with the WWEs in GL and WA, and the WDEs in EU, SC and USGP. Shadings represent the daily composite anomaly values of (I-V) latent heat flux (units: W m^{-2}), (VI-X) sensible heat flux (units: W m^{-2}), (XI-XV) downward short-wave radiation (units: W m^{-2}), (XVI-XX) net short-wave radiation (units: W m^{-2}), (XXI-XXV) downward long-wave radiation (units: W m^{-2}), and (XXVI-XXX) net long-wave radiation (units: W m^{-2}). The gray dots indicate the areas where the anomalies are statistically significant at the 95% confidence level.

Larger anomalies of latent heat flux and sensible heat flux occur during WDEs over EU, SC, and USGP than during WWEs over GL and WA (Fig. 4). Previous studies have suggested that the land-atmosphere interaction significantly contributes to the occurrence of WDEs, particularly to the lengthening of these events (Libonati et al., 2022; Miralles et al., 2019; Seo & Ha, 2022; Zhang et al., 2020). We calculate the coupling metric to compare the strength of land-atmosphere interaction during WWEs and WDEs. The positive coupling metric over non-ice-covered regions indicates that the land-atmosphere interaction is indeed active during WDEs (Figs. 5c-5e). Under the control of high-pressure systems (HPs), the non-ice-covered surface is evaporated to dryness by diabatic warming of subsidence motions and excessive downward SWR, and it fails to be re-hydrated due to the lack of precipitation. The resultant soil moisture deficiency (Figs. 5h-5j)

allows the surface to heat more quickly due to attenuated evaporation, and enhances upward sensible heat flux that warms the overlying air. This process further strengthens the existing HPs above, which exacerbates surface dry conditions in turn. Thus, a positive feedback loop to trigger and maintain WDEs is established, explaining why prolonged compound warm events tend to occur over non-ice-covered zones.

However, surface turbulent heat fluxes are nearly shut off over the ice-covered regions. Since deep HPs are commonly thermally maintained, their centers tend to be located above the warmer oceanic surface away from the ice-covered regions, situating the ice sheets on their fringes. As a result, these deep HPs induce warm-moist air intrusions by horizontal advective motions and thus result in the high prevalence of WWEs over the polar ice sheets.

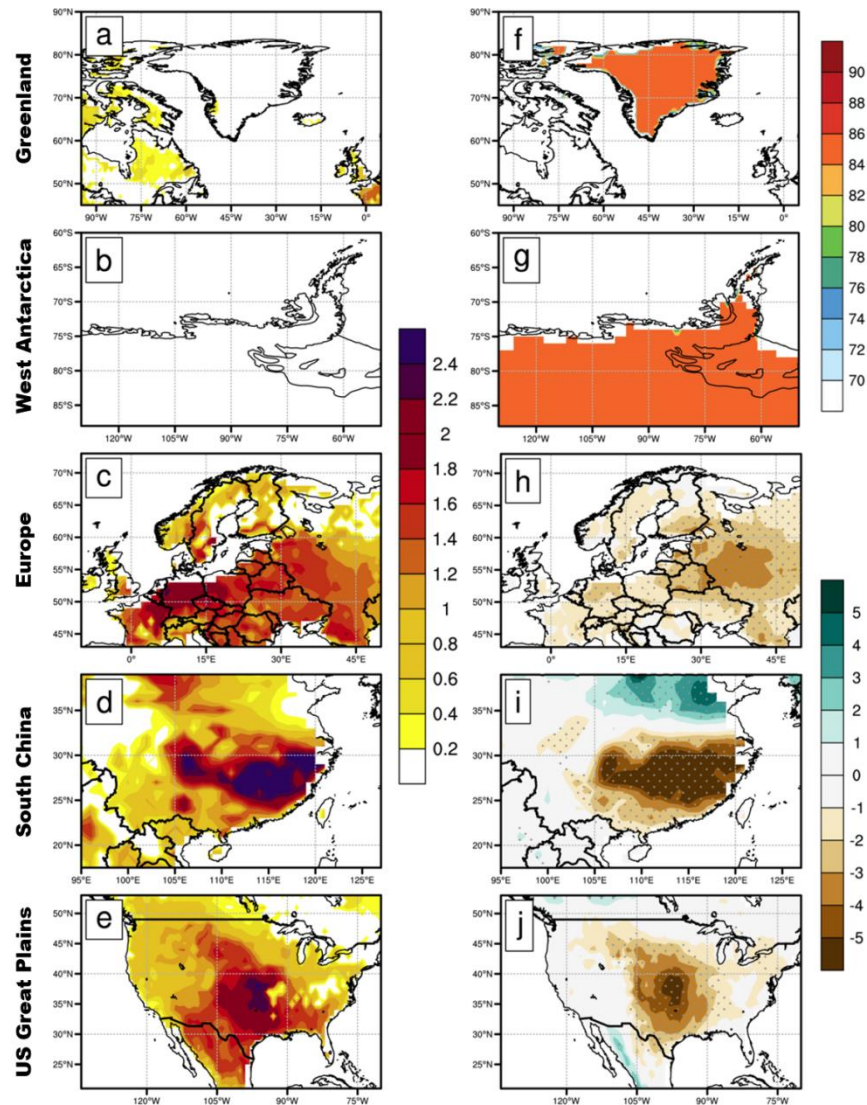


Figure 5. Land-atmosphere interaction associated with the WWEs in GL and WA, and the WDEs in EU, SC and USGP. Shadings represent the daily composite values of (a-e) coupling metric, (f, g) surface albedo (units: %), and (h, i, j) soil moisture anomalies (units: $10^{-2} \text{ m}^3 \text{ m}^{-3}$). Gray dots indicate the areas where soil moisture anomalies are statistically significant at the 95% confidence level.

4 Conclusions

In this study, we reveal the physical mechanisms for a paradigm shift in compound extreme warm events from extra-polar regions to ice-covered polar regions. Warm-wet events (WWEs) and warm-dry events (WDEs), the two different types of compound warm events, are defined by the joint percentile thresholds of 2-m temperature and precipitation. WDEs, which possess a longer duration, prevail in non-ice-covered zones, while WWEs, with a shorter duration, predominate in ice-covered regions. Both WWEs and WDEs are driven by anomalous high-pressure systems (HPs), but they experience distinct local dynamic processes. By comparing the physical mechanisms for compound warm events in Greenland, West Antarctica, Europe, South China, and the US Great Plains, we conclude that the shift in the paradigm results from a combination of attenuation in land-atmosphere interaction and transformation in the dynamic processes controlled by HPs.

The local dynamic processes and surface energy responses controlled by HPs during WWEs and WDEs are summarized in the schematic diagram as shown in Fig. 6. In the non-ice-covered zones, a strong land-atmosphere feedback loop initiated by HPs prompts heatwaves to coincide with extreme dry conditions. The presence of HPs creates a relatively dry condition with clear skies, allowing for more shortwave radiation to strike the surface and resulting in a warmer surface. The heat is then lost via longwave radiation from the surface, and surface sensible and latent heat fluxes to the air, which leads to a decrease in soil moisture. The extreme dry condition reinforces warmer conditions through active land-atmosphere interaction, intensifying and prolonging the warm spell.

In the ice-covered regions, local dynamic processes and land-air interaction created by HPs are different from those in the non-ice-covered zones. The WWEs over the ice sheet are sustained by horizontal warm and moist air intrusions. When warm air encounters the ice sheet, the surface is directly warmed by longwave radiation, while the air cools down, leading to increased cloud cover.

The abundant clouds can trap more longwave radiation between the surface and the clouds due to their longwave effect but reduce shortwave radiation to the surface. Simultaneously, more clouds over the ice sheet can lead to more precipitation. These physical processes are responsible for the high prevalence of WWEs. Specifically, the ice cover acts as a barrier that dampens land-atmosphere interaction, resulting in a relatively shorter duration of WWEs.

An improved understanding of the paradigm shift of compound extreme events from extra-polar regions to polar regions would enable us to make more accurate projections of climate changes in each region and assess relative climate risks. It should be noted that the contribution of WWEs to ice sheets could be either positive (solid precipitation) or negative (liquid precipitation). Under the backdrop of global warming, the frequency of liquid precipitation increases, which poses a larger threat from WWEs to the ice sheet. Unlike solid precipitation, liquid precipitation can directly infiltrate the ice sheet, leading to enhanced melting and potential destabilization. This heightened risk of liquid precipitation exacerbates the vulnerability of the cryosphere to the impact of WWEs, underscoring the urgent need for further investigations and proactive measures to mitigate the potential consequence on polar ice sheets.

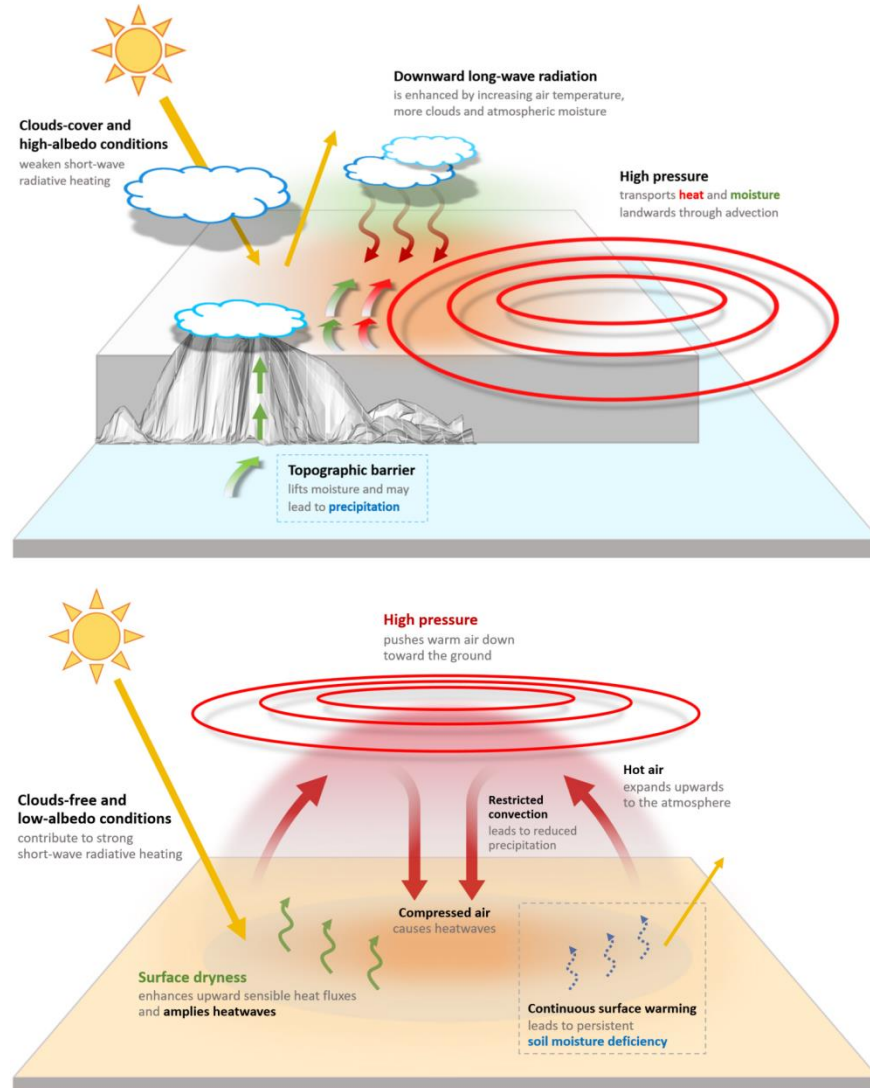


Figure 6. Schematic diagram illustrating the WDEs (top) over the ice-covered surface and the WDEs (bottom) above the non-ice-covered surface.

298 Acknowledgment

299 This research is supported by the Guangdong Major Project of Basic and Applied Basic
300 Research (2020B0301030004) and the National Natural Science Foundation of China
301 (42075028).

302

303 Open Research

304 The ERA5 reanalysis used in this study is available from
305 <https://doi.org/10.24381/cds.adbb2d47> and <https://doi.org/10.24381/cds.bd0915c6>.

References

- Afroz, M., Chen, G., & Anandhi, A. (2023). Drought- and heatwave-associated compound extremes: A review of hotspots, variables, parameters, drivers, impacts, and analysis frameworks. *Frontiers in Earth Science*, 10, 914437. <https://doi.org/10.3389/feart.2022.914437>
- Bakker, P., Schmittner, A., Lenaerts, J. T. M., Abe-Ouchi, A., Bi, D., Van Den Broeke, M. R., Chan, W. -L., Hu, A., Beadling, R. L., Marsland, S. J., Mernild, S. H., Saenko, O. A., Swingedouw, D., Sullivan, A., & Yin, J. (2016). Fate of the Atlantic Meridional Overturning Circulation: Strong decline under continued warming and Greenland melting. *Geophysical Research Letters*, 43(23). <https://doi.org/10.1002/2016GL070457>
- Barriopedro, D., García-Herrera, R., Ordóñez, C., Miralles, D. G., & Salcedo-Sanz, S. (2023). Heat waves: Physical understanding and scientific challenges. *Reviews of Geophysics*, 61(2), e2022RG000780. <https://doi.org/10.1029/2022RG000780>
- Beniston, M. (2009). Trends in joint quantiles of temperature and precipitation in Europe since 1901 and projected for 2100. *Geophysical Research Letters*, 36(7), 2008GL037119. <https://doi.org/10.1029/2008GL037119>
- Bintanja, R. (2018). The impact of Arctic warming on increased rainfall. *Scientific Reports*, 8(1), 16001. <https://doi.org/10.1038/s41598-018-34450-3>
- Cai, Z., You, Q., Chen, H. W., Zhang, R., Zuo, Z., Chen, D., Cohen, J., & Screen, J. A. (2024). Assessing Arctic wetting: Performances of CMIP6 models and projections of precipitation changes. *Atmospheric Research*, 297, 107124. <https://doi.org/10.1016/j.atmosres.2023.107124>
- Clem, K. R., Adusumilli, S., Baiman, R., Banwell, A. F., Barreira, S., Beadling, R. L., Bozkurt, D., Colwell, S., Coy, L., Datta, R. T., Laat, J. D., Plessis, M. du, Dunmire, D., Fogt, R. L., Freeman, N. M., Fricker, H. A., Gardner, A. S., Gille, S. T., Johnson, B., ... Veasey, S. W. (2023). Antarctica and the Southern Ocean. *Bulletin of the American Meteorological Society*, 104(9), S322–S365. <https://doi.org/10.1175/BAMS-D-23-0077.1>
- Deb, P., Orr, A., Hosking, J. S., Phillips, T., Turner, J., Bannister, D., Pope, J. O., & Colwell, S. (2016). An assessment of the Polar Weather Research and Forecasting (WRF) model

- 335 representation of near-surface meteorological variables over West Antarctica. *Journal of*
 336 *Geophysical Research: Atmospheres*, 121(4), 1532–1548.
 337 <https://doi.org/10.1002/2015JD024037>
- 338 DeConto, R. M., & Pollard, D. (2016). Contribution of Antarctica to past and future sea-level rise.
 339 *Nature*, 531(7596), 591–597. <https://doi.org/10.1038/nature17145>
- 340 Djoumna, G., & Holland, D. M. (2021). Atmospheric rivers, warm air intrusions, and surface
 341 radiation balance in the Amundsen Sea Embayment. *Journal of Geophysical Research:*
 342 *Atmospheres*, 126(13), e2020JD034119. <https://doi.org/10.1029/2020JD034119>
- 343 Earth, B. (2022). *Antarctic heatwave: A rapid analysis of the March 2022 Dome C record*
 344 *heatwave*. Retrieved from
 345 [https://berkeleyearth.wpengine.com/antarctic-heatwave-rapid-attribution-review-dome-c-](https://berkeleyearth.wpengine.com/antarctic-heatwave-rapid-attribution-review-dome-c-record/)
 346 [record/](https://berkeleyearth.wpengine.com/antarctic-heatwave-rapid-attribution-review-dome-c-record/)
- 347 Feng, S., Hao, Z., Zhang, X., & Hao, F. (2019). Probabilistic evaluation of the impact of
 348 compound dry-hot events on global maize yields. *Science of the Total Environment*, 689,
 349 1228–1234. <https://doi.org/10.1016/j.scitotenv.2019.06.373>
- 350 Feron, S., Cordero, R. R., Damiani, A., Malhotra, A., Seckmeyer, G., & Llanillo, P. (2021).
 351 Warming events projected to become more frequent and last longer across Antarctica.
 352 *Scientific Reports*, 11(1), 19564. <https://doi.org/10.1038/s41598-021-98619-z>
- 353 Gao, Y., Liu, J., Wen, Q., Chen, D., Sun, W., Ning, L., & Yan, M. (2024). The influence of
 354 increased CO₂ concentrations on AMOC interdecadal variability under the LGM
 355 background. *Journal of Geophysical Research: Atmospheres*, 129(3), e2023JD039976.
 356 <https://doi.org/10.1029/2023JD039976>
- 357 González-Herrero, S., Barriopedro, D., Trigo, R. M., López-Bustins, J. A., & Oliva, M. (2022).
 358 Climate warming amplified the 2020 record-breaking heatwave in the Antarctic Peninsula.
 359 *Communications Earth & Environment*, 3(1), 1–9.
 360 <https://doi.org/10.1038/s43247-022-00450-5>
- 361 Gorodetskaya, I. V., Durán-Alarcón, C., González-Herrero, S., Clem, K. R., Zou, X., Rowe, P.,
 362 Rodríguez Imazio, P., Campos, D., Leroy-Dos Santos, C., Dutrievoz, N., Wille, J. D.,
 363 Chyhareva, A., Favier, V., Blanchet, J., Pohl, B., Cordero, R. R., Park, S.-J., Colwell, S.,

- 364 Lazzara, M. A., ... Picard, G. (2023). Record-high Antarctic Peninsula temperatures and
365 surface melt in February 2022: A compound event with an intense atmospheric river. *Npj*
366 *Climate and Atmospheric Science*, 6(1), 202. <https://doi.org/10.1038/s41612-023-00529-6>
- 367 Han, Q., Xu, W., & Shi, P. (2022). Mapping global population exposure to heatwaves. In *Atlas of*
368 *Global Change Risk of Population and Economic Systems* (pp. 95–102). Springer Nature.
369 https://doi.org/10.1007/978-981-16-6691-9_6
- 370 Hao, Z., Hao, F., Singh, V. P., Xia, Y., Shi, C., & Zhang, X. (2018). A multivariate approach for
371 statistical assessments of compound extremes. *Journal of Hydrology*, 565, 87–94.
372 <https://doi.org/10.1016/j.jhydrol.2018.08.025>
- 373 Hao, Z., Hao, F., Xia, Y., Feng, S., Sun, C., Zhang, X., Fu, Y., Hao, Y., Zhang, Y., & Meng, Y.
374 (2022). Compound droughts and hot extremes: Characteristics, drivers, changes, and
375 impacts. *Earth-Science Reviews*, 235, 104241.
376 <https://doi.org/10.1016/j.earscirev.2022.104241>
- 377 He, Y., Fang, J., Xu, W., & Shi, P. (2022). Substantial increase of compound droughts and
378 heatwaves in wheat growing seasons worldwide. *International Journal of Climatology*,
379 42(10), 5038–5054. <https://doi.org/10.1002/joc.7518>
- 380 Hersbach, H., Bell, B., Berrisford, P., Hirahara, S., Horányi, A., Muñoz-Sabater, J., Nicolas, J.,
381 Peubey, C., Radu, R., Schepers, D., Simmons, A., Soci, C., Abdalla, S., Abellan, X.,
382 Balsamo, G., Bechtold, P., Biavati, G., Bidlot, J., Bonavita, M., ... Thépaut, J.-N. (2020).
383 The ERA5 global reanalysis. *Quarterly Journal of the Royal Meteorological Society*,
384 146(730), 1999–2049. <https://doi.org/10.1002/qj.3803>
- 385 Holmes, A., Rüdiger, C., Mueller, B., Hirschi, M., & Tapper, N. (2017). Variability of soil
386 moisture proxies and hot days across the climate regimes of Australia. *Geophysical*
387 *Research Letters*, 44(14), 7265–7275. <https://doi.org/10.1002/2017GL073793>
- 388 Hu, X., Sejas, S. A., Cai, M., Li, Z., & Yang, S. (2019). Atmospheric dynamics footprint on the
389 January 2016 ice sheet melting in West Antarctica. *Geophysical Research Letters*, 46(5),
390 2829–2835. <https://doi.org/10.1029/2018GL081374>
- 391 Jiang, N., Zhu, C., Hu, Z.-Z., McPhaden, M. J., Chen, D., Liu, B., Ma, S., Yan, Y., Zhou, T., Qian,
392 W., Luo, J., Yang, X., Liu, F., & Zhu, Y. (2024). Enhanced risk of record-breaking regional

- temperatures during the 2023–24 El Niño. *Scientific Reports*, 14(1), 2521.
<https://doi.org/10.1038/s41598-024-52846-2>
- Leeson, A. A., Eastoe, E., & Fettweis, X. (2018). Extreme temperature events on Greenland in observations and the MAR regional climate model. *The Cryosphere*, 12(3), 1091–1102.
<https://doi.org/10.5194/tc-12-1091-2018>
- Li, W., Wu, Y., & Hu, X. (2023). The processes-based attributes of four major surface melting events over the Antarctic Ross ice shelf. *Advances in Atmospheric Sciences*, 40(9), 1662–1670. <https://doi.org/10.1007/s00376-023-2287-3>
- Libonati, R., Geirinhas, J. L., Silva, P. S., Russo, A., Rodrigues, J. A., Belém, L. B. C., Nogueira, J., Roque, F. O., DaCamara, C. C., Nunes, A. M. B., Marengo, J. A., & Trigo, R. M. (2022). Assessing the role of compound drought and heatwave events on unprecedented 2020 wildfires in the Pantanal. *Environmental Research Letters*, 17(1), 015005.
<https://doi.org/10.1088/1748-9326/ac462e>
- Liu, Z., & Zhou, W. (2023a). Global seasonal-scale meteorological droughts. Part I: Detection, metrics, and inland/coastal types. *Ocean-Land-Atmosphere Research*, 2, 0016.
<https://doi.org/10.34133/olar.0016>
- Liu, Z., & Zhou, W. (2023b). Global seasonal-scale meteorological droughts. Part II: Temperature anomaly-based classifications. *Ocean-Land-Atmosphere Research*, 2, 0017.
<https://doi.org/10.34133/olar.0017>
- Mattingly, K. S., Mote, T. L., Fettweis, X., As, D. van, Tricht, K. V., Lhermitte, S., Pettersen, C., & Fausto, R. S. (2020). Strong summer atmospheric rivers trigger Greenland ice sheet melt through spatially varying surface energy balance and cloud regimes. *Journal of Climate*, 33(16), 6809–6832. <https://doi.org/10.1175/JCLI-D-19-0835.1>
- McNeall, D., Halloran, P. R., Good, P., & Betts, R. A. (2011). Analyzing abrupt and nonlinear climate changes and their impacts. *WIREs Climate Change*, 2(5), 663–686.
<https://doi.org/10.1002/wcc.130>
- Miralles, D. G., Gentile, P., Seneviratne, S. I., & Teuling, A. J. (2019). Land–atmospheric feedbacks during droughts and heatwaves: State of the science and current challenges.

- 421 *Annals of the New York Academy of Sciences*, 1436(1), 19–35.
 422 <https://doi.org/10.1111/nyas.13912>
- 423 Miralles, D. G., Van Den Berg, M. J., Teuling, A. J., & De Jeu, R. A. M. (2012). Soil moisture-
 424 temperature coupling: A multiscale observational analysis. *Geophysical Research Letters*,
 425 39(21), 2012GL053703. <https://doi.org/10.1029/2012GL053703>
- 426 Mueller, B., & Seneviratne, S. I. (2012). Hot days induced by precipitation deficits at the global
 427 scale. *Proceedings of the National Academy of Sciences*, 109(31), 12398–12403.
 428 <https://doi.org/10.1073/pnas.1204330109>
- 429 Mukherjee, S., Ashfaq, M., & Mishra, A. K. (2020). Compound drought and heatwaves at a global
 430 scale: The role of natural climate variability-associated synoptic patterns and land-surface
 431 energy budget anomalies. *Journal of Geophysical Research: Atmospheres*, 125(11),
 432 e2019JD031943. <https://doi.org/10.1029/2019JD031943>
- 433 Nicolas, J. P., & Bromwich, D. H. (2011). Climate of West Antarctica and influence of marine air
 434 intrusions. *Journal of Climate*, 24(1), 49–67. <https://doi.org/10.1175/2010JCLI3522.1>
- 435 Pohl, B., Favier, V., Wille, J., Udy, D. G., Vance, T. R., Pergaud, J., Dutrievoz, N., Blanchet, J.,
 436 Kittel, C., Amory, C., Krinner, G., & Codron, F. (2021). Relationship between weather
 437 regimes and atmospheric rivers in East Antarctica. *Journal of Geophysical Research:*
 438 *Atmospheres*, 126(24), e2021JD035294. <https://doi.org/10.1029/2021JD035294>
- 439 Ridder, N. N., Pitman, A. J., & Ukkola, A. M. (2021). Do CMIP6 climate models simulate global
 440 or regional compound events skillfully? *Geophysical Research Letters*, 48(2),
 441 e2020GL091152. <https://doi.org/10.1029/2020GL091152>
- 442 Ridder, N. N., Pitman, A. J., Westra, S., Ukkola, A., Do, H. X., Bador, M., Hirsch, A. L., Evans, J.
 443 P., Di Luca, A., & Zscheischler, J. (2020). Global hotspots for the occurrence of compound
 444 events. *Nature Communications*, 11(1), 5956.
 445 <https://doi.org/10.1038/s41467-020-19639-3>
- 446 Rignot, E., Velicogna, I., Van Den Broeke, M. R., Monaghan, A., & Lenaerts, J. T. M. (2011).
 447 Acceleration of the contribution of the Greenland and Antarctic ice sheets to sea level rise:
 448 Acceleration of ice sheet loss. *Geophysical Research Letters*, 38(5), n/a-n/a.
 449 <https://doi.org/10.1029/2011GL046583>

- Salvador, C., Nieto, R., Vicente-Serrano, S. M., García-Herrera, R., Gimeno, L., & Vicedo-Cabrera, A. M. (2023). Public health implications of drought in a climate change context: A critical review. *Annual Review of Public Health*, 44(1), 213–232. <https://doi.org/10.1146/annurev-publhealth-071421-051636>
- Seo, Y.-W., & Ha, K.-J. (2022). Changes in land-atmosphere coupling increase compound drought and heatwaves over northern East Asia. *Npj Climate and Atmospheric Science*, 5(1), 100. <https://doi.org/10.1038/s41612-022-00325-8>
- Shields, C. A., Wille, J. D., Marquardt Collow, A. B., MacLennan, M., & Gorodetskaya, I. V. (2022). Evaluating uncertainty and modes of variability for Antarctic atmospheric rivers. *Geophysical Research Letters*, 49(16), e2022GL099577. <https://doi.org/10.1029/2022GL099577>
- Tripathy, K. P., & Mishra, A. K. (2023). How unusual is the 2022 European compound drought and heatwave event? *Geophysical Research Letters*, 50(15), e2023GL105453. <https://doi.org/10.1029/2023GL105453>
- van der Schot, J., Abermann, J., Silva, T., Jensen, C. D., Noël, B., & Schöner, W. (2023). Precipitation trends (1958–2021) on Ammassalik island, south-east Greenland. *Frontiers in Earth Science*, 10. <https://doi.org/10.3389/feart.2022.1085499>
- Vignon, É., Roussel, M.-L., Gorodetskaya, I. V., Genthon, C., & Berne, A. (2021). Present and future of rainfall in Antarctica. *Geophysical Research Letters*, 48(8), e2020GL092281. <https://doi.org/10.1029/2020GL092281>
- Wang, S., Ding, M., Liu, G., Zhao, S., Zhang, W., Li, X., Chen, W., Xiao, C., & Qin, D. (2023). New record of explosive warmings in East Antarctica. *Science Bulletin*, 68(2), 129–132. <https://doi.org/10.1016/j.scib.2022.12.013>
- Wille, J. D., Alexander, S. P., Amory, C., Baiman, R., Barthélemy, L., Bergstrom, D. M., Berne, A., Binder, H., Blanchet, J., Bozkurt, D., Bracegirdle, T. J., Casado, M., Choi, T., Clem, K. R., Codron, F., Datta, R., Battista, S. D., Favier, V., Francis, D., ... Zou, X. (2024). The extraordinary March 2022 East Antarctica “heat” wave. Part II: Impacts on the Antarctic ice sheet. *Journal of Climate*, 37(3), 779–799. <https://doi.org/10.1175/JCLI-D-23-0176.1>

- Xu, L., Zhang, T., Yu, W., & Yang, S. (2023). Changes in concurrent precipitation and temperature extremes over the Asian monsoon region: Observation and projection. *Environmental Research Letters*, 18(4), 044021. <https://doi.org/10.1088/1748-9326/acbfd0>
- Xu, M., Yang, Q., Hu, X., Liang, K., & Vihma, T. (2022). Record-breaking rain falls at Greenland summit controlled by warm moist-air intrusion. *Environmental Research Letters*, 17(4), 044061. <https://doi.org/10.1088/1748-9326/ac60d8>
- Yang, R., Hu, X., Cai, M., Deng, Y., Clem, K., Yang, S., Xu, L., & Yang, Q. (2024). A paradigm shift of compound extremes over polar ice sheets. *Ocean-Land-Atmosphere Research*, 3, 0040. <https://doi.org/10.34133/olar.0040>
- Yang, X., Shen, C., Zhang, G., & Chen, D. (2024). Enhanced spring warming of the Tibetan Plateau amplifies summer heat stress in eastern Europe. *Climate Dynamics*. <https://doi.org/10.1007/s00382-024-07197-z>
- Yang, X., Zeng, G., Zhang, S., Iyakaremye, V., Shen, C., Wang, W.-C., & Chen, D. (2024). Phase-locked Rossby wave-4 pattern dominates the 2022-like concurrent heat extremes across the Northern Hemisphere. *Geophysical Research Letters*, 51(4), e2023GL107106. <https://doi.org/10.1029/2023GL107106>
- Zhang, P., Jeong, J.-H., Yoon, J.-H., Kim, H., Wang, S.-Y. S., Linderholm, H. W., Fang, K., Wu, X., & Chen, D. (2020). Abrupt shift to hotter and drier climate over inner East Asia beyond the tipping point. *Science*, 370(6520), 1095–1099. <https://doi.org/10.1126/science.abb3368>
- Zhang, T., Deng, Y., Chen, J., Yang, S., & Dai, Y. (2023). An energetics tale of the 2022 mega-heatwave over central-eastern China. *Npj Climate and Atmospheric Science*, 6(1), 162. <https://doi.org/10.1038/s41612-023-00490-4>
- Zhu, J., Liu, Z., Zhang, X., Eisenman, I., & Liu, W. (2014). Linear weakening of the AMOC in response to receding glacial ice sheets in CCSM3. *Geophysical Research Letters*, 41(17), 6252–6258. <https://doi.org/10.1002/2014GL060891>

505 Zou, X., Bromwich, D. H., Montenegro, A., Wang, S., & Bai, L. (2021). Major surface melting
506 over the Ross Ice Shelf. Part I: Foehn effect. *Quarterly Journal of the Royal*
507 *Meteorological Society*, 147(738), 2874–2894. <https://doi.org/10.1002/qj.4104>

508 Zscheischler, J., & Seneviratne, S. I. (2017). Dependence of drivers affects risks associated with
509 compound events. *Science Advances*, 3(6), e1700263.
510 <https://doi.org/10.1126/sciadv.1700263>

511